Octahedral tilt-suppression of ferroelectric domain wall dynamics and the associated piezoelectric activity in $Pb(Zr,Ti)O_3$

R. Eitel* and C. A. Randall
Materials Research Institute, The Pennsylvania State University, University Park, Pennsylvania 16802, USA
(Received 19 June 2006; revised manuscript received 15 January 2007; published 12 March 2007)

The *R*3*m*-*R*3*c* transition is in a limited phase field in the $Pb(Zr_{1-x},Ti_x)O_3$ (PZT) phase diagram and is a ferroelectric-ferroelectric phase transition that involves the coupling of a secondary displacive ferroelastic phase transition, associated with a structural rotation of the octahedra about the polar threefold axis. Through systematic temperature-dependent piezoelectric characterization under resonance conditions and high-field unipolar ac drive the influence of the aforementioned transition on piezoelectric and electromechanical properties is noted for two compositions $x=0.30$ and $x=0.40$ mol fraction lead titanate. Applying Rayleigh law analysis to access the relative extrinsic domain wall contributions to the nonlinear permittivity and converse piezoelectric properties, we observe significant differences in the nonlinear response between the *R*3*m* and *R*3*c* phases and note a discontinuity at the transition for both PZT compositions. A complementary study was conducted through diffraction contrast transmission electron microscopy to access structure property relations. Diffraction contrast imaging reveals that antiphase boundaries (APB's) associated with octahedral tilt may coincide with non-180° ferroelectric domain walls. This microstructural evidence suggests that APB's suppress the motion of non-180° ferroelectric domain walls, leading to reduced extrinsic contributions to the piezoelectric and dielectric response in the low-temperature phase (*R*3*c*). The implications of these observations are discussed in relation to both the PZT system and other perovskite-based systems such as $BiMO_3$-$PbTiO_3$ systems.

DOI: 10.1103/PhysRevB.75.094106 PACS number(s): 77.84.Dy, 77.65.−j, 77.80.Dj

I. INTRODUCTION

The perovskite crystal structure plays host to a wide range of electronic phenomena including ferroelectricity, ferromagnetism, superconductivity, semiconductivity, metallic conductivity, and Mott-insulator transitions.[1,2] Perovskite compositions that are ferroelectric can be poled to obtain piezoelectric properties. The poling process involves the application of an electric field to align the local spontaneous polarization through domain switching, resulting in a bulk net remnant polarization (P_r). The efficiency of the poling process and piezoelectric properties is largely dependent on the crystallographic phase and the related domain structure. The extrinsic domain contributions to the dielectric and piezoelectric properties may comprise greater than 70% of total response of high-performance piezoelectric ceramics.[3–9]

Most high-performance commercial piezoelectric ceramic compositions are based on the solid solutions between $Pb(Zr_{1-x},Ti_x)O_3$ (PZT) near the largely temperature-independent or morphotropic phase boundary (MPB) between rhombohedral and tetragonal ferroelectric phases.[10,11] Detailed structural analysis of PZT near the MPB reveals a monoclinic ferroelectric phase in a narrow compositional range at temperatures below room temperature.[12] On further cooling a monoclinic (*Cm*)-monoclinic (*Cc*) transition occurs to an octahedrally tilted phase.[13,14] Physically, the octahedral transition is due to the rotation of the octahedra comprising the oxygen anion sublattice. In the low-temperature phase at the MPB, tilting occurs due to a coupling with the phase transition in the rhombohedral ferroelectric phase. The rhombohedral phase transition is between *R*3*m* and *R*3*c*, and the transition temperature (T_{tilt}) is dependent on the Zr/Ti ratio.[10,15] This tilt transition is driven by an antidistortive soft-mode condensation.[16] In the tilted phase, oxygen octahedra are rotated around the [111] direction in an alternating clockwise-anticlockwise sequence. In the classification system described by Glazer this tilt system is assigned the notation ($a^-a^-a^-$), indicating rotations of equal magnitude (a) and alternating in direction ($^-$) about each of the u, v, w lattice directions.[17–19] This results in a doubling of the unit cell lattice parameter in the *R*3*c* phase; this structure is illustrated schematically (CaRIne) in Fig. 1.

The objective of this investigation is to study and quantify the impact of the onset of the tilt transition on the extrinsic and high-field piezoelectric properties. Others have noted the

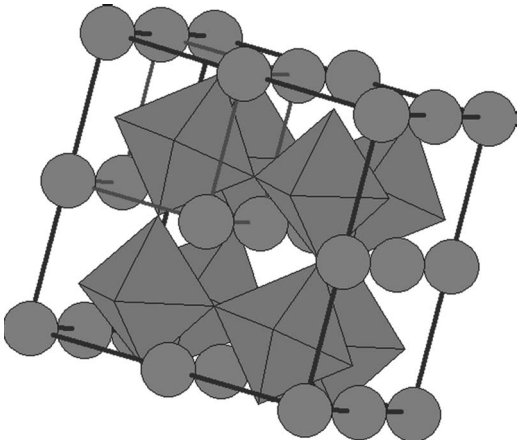

FIG. 1. The unit cell of the *R*3*c* tilted perovskite phase consisting of four perovskite formula units. The lead ions are indicated at the cube corners while the (Ti and Zr) cations (not visible) would be found at the center of the octahedra; the octahedra are drawn with the oxygen anions removed for clarity.

ability to suppress the piezoelectric response by inducing a tilted phase through Sr additions in optimized MPB PZT compositions.[20,21] However, direct investigation of tilt at the MPB is difficult owing to the fact that application of large electric fields may induce a phase transition between the rhombohedral and tetragonal phases. Furthermore, the monoclinic phases are difficult to detect, due to their narrow compositional and temperature range. To limit these experimental complexities in determining the influence of octahedral tilt on piezoelectric activity, this study was conducted on unmodified compositions in rhombohedral PZT over a large temperature range covering the transition between the *R*3*c* and *R*3*m* ferroelectric phases.

The symmetry and domain structure of the *R*3*c* and *R*3*m* PZT phases and their associated electrical properties have been characterized by a number of authors.[10,13,15,22–24] In the current approach Rayleigh analysis, high-field piezoelectric strain, and low-field electromechanical characterization will be combined with *in situ* transmission electron microscopy (TEM) to investigate the properties and structure associated with the $R3m \rightarrow R3c$ tilt transition. From this study, we will unequivocally demonstrate that extrinsic piezoelectric activity is strongly clamped by octahedral tilt transitions limiting the piezoelectric performance in the tilted phase. We will discuss the details of this clamping and point out important implications for the compositional development of new perovskite-based piezoelectrics.

II. EXPERIMENT

A. Processing

Lead zirconate titanate $Pb(Zr_{1-x},Ti_x)O_3$ powders were prepared with $x=30$ and 40 mol % titanium corresponding to compositions with room-temperature space groups *R*3*c* and *R*3*m*, respectively. Powders were prepared using the traditional solid-state ceramic processing route. Raw materials of lead carbonate $PbCO_3$ (White Lead, Hammond Lead Products), titanium dioxide (Ishihara Corporation), and zirconium dioxide (Alfa Aesar) were batched to achieve the desired composition. Aqueous powder suspensions, containing a dispersant (Darvan 821A, RT Vanderbilt Company, Inc.), were vibratory milled using yttria-stabilized zirconia media for 20 h. Suspensions were thoroughly dried at 200 °C. Then 3 wt % binder (Acryloid, Rhom and Haas Co.) was added before crushing and hand grinding aggregates to pass through a 200-mesh screen. Pellets were uniaxially pressed at 20 000 psi, then isostatically pressed at 30 000 psi. Binder burnout was conducted on open trays at 500 °C. Pellets were sintered in covered crucibles using a lead zirconate source powder at 1150 °C for 2 h. Samples were greater than 98% dense by immersion determination and x-ray diffraction of crushed pellets confirmed phase pure perovskite structure.

B. Electrical characterization

Fired pellets for electrical characterization were ground to 1 mm thickness and electroded with fired on silver ink (6160, Dupont). All samples were poled at room temperature and 40 kV/cm and allowed to age 24 h before measuring.

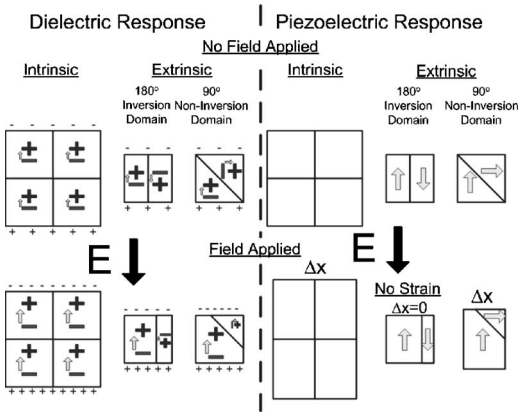

FIG. 2. The schematic illustration of the dielectric and piezoelectric response in ferroelectric materials. The intrinsic response is shown to be associated with the single domain response arising from the polarizability of the crystal lattice, leading to both a linear dielectric displacement and net strain response. The extrinsic contribution is associated with the motion of ferroelectric domain walls preferentially enhancing the fraction of domains most nearly aligned with the applied field. Note that there is no net strain contribution due to 180° inversion domains.

Low-field piezoelectric properties were measured from disk samples using an impedance analyzer (4194A, Agilent Inc.) following the electromechanical resonance technique (IEEE Std 176-1987). High-field unipolar polarization and strain loops were obtained using a modified Sawyer-Tower circuit incorporating a linear variable differential transducer (LVDT) for strain data. *In situ* electromechanical properties were measured in an environmental chamber containing a bath of dielectric fluid (Galden, Solvay Solexis) to prevent arcing across the pellet edges. This fixture was also used for measurement of minor hysteresis loops for Rayleigh analysis.

C. Rayleigh technique for characterization of extrinsic response

It is well known that the dielectric and piezoelectric response in ferroelectrics contains both intrinsic and extrinsic contributions. The intrinsic response refers to the atomic lattice contributions at the unit cell level. The extrinsic response refers to contributions due to movement of domain walls. Under an applied electrical field, domain wall motion increases the volume fraction of domain variants most closely aligned to the applied field at the expense of other variants. Figure 2 illustrates both the intrinsic and extrinsic components of the polarization and strain response due to an applied electric field.[8,9,25] As indicated, the motion of noninversion (non-180°) domain walls contributes to both the dielectric and piezoelectric response. However, inversion-type (180°) domain wall motion contributes only to the dielectric response, due to the equivalent strain state in oppositely polarized domains. In *R*3*m* perovskite ferroelectrics the noninversion domains are twinned on $\{100\}_c$ and $\{110\}_c$ crystallographic planes (relative to the pseudocubic structure, denoted "$\{hkl\}_c$").[26] The Rayleigh parameters were calcu-

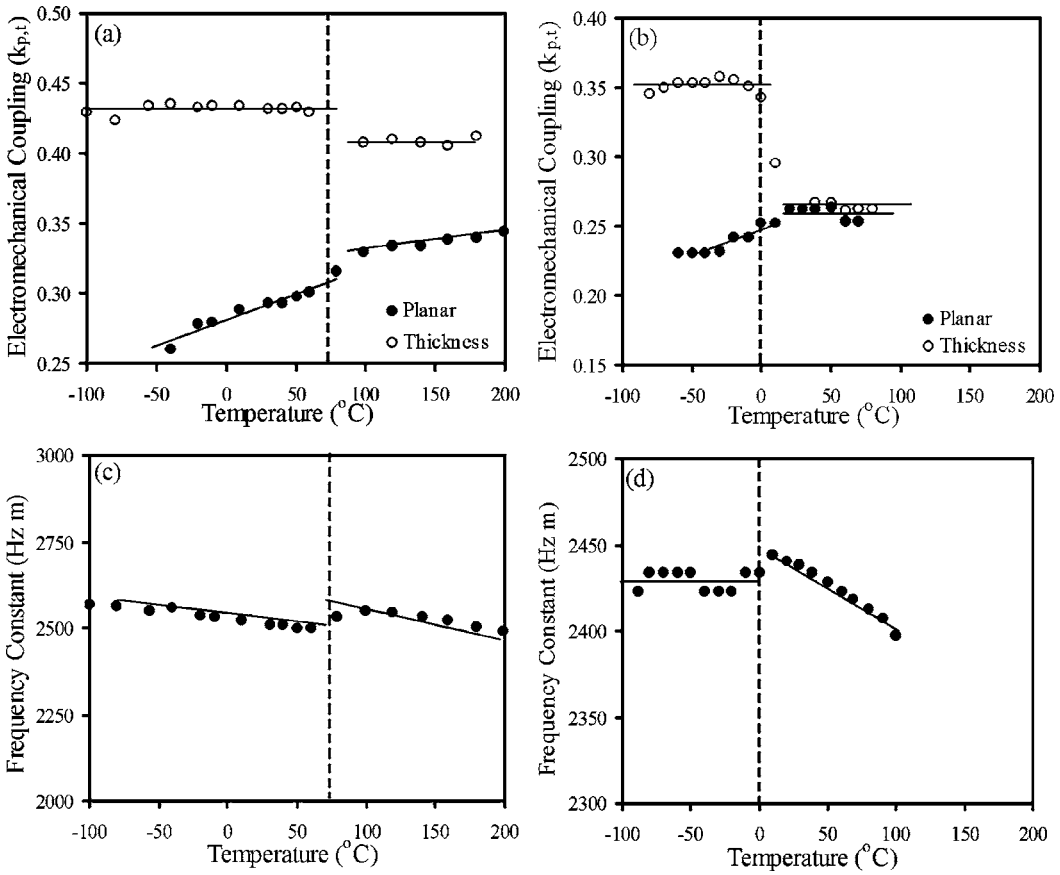

FIG. 3. Low-field electromechanical resonance response for $Pb(Zr_x,Ti_{1-x})O_3$ with 30 (a), (c) and 40 (b), (d) mol % titanium content.

lated from linear portions of the field dependence of the real permittivity and real piezoelectric response at 1 Hz over the temperature range $-150 < T < 180$ °C.

The movement of the domain walls under a cyclic driving electric field is an irreversible and lossy process, and therefore the associated responses are complex properties with real and imaginary components:

$$\varepsilon^* = \varepsilon'_{int} + \varepsilon'_{ext} + i\varepsilon''_{\text{ext}}, \tag{1}$$

$$d^* = d'_{int} + d'_{ext} + id''_{ext}, \tag{2}$$

where ε^* and d^* are the complex dielectric permittivity and piezoelectric response; the real response contains both intrinsic and extrinsic components (ε'_{int}, ε'_{ext}, d'_{int}, d'_{ext}) and the complex response is dominated by extrinsic contributions (e''_{ext}, d''_{ext}). It has been shown phenomenologically that both the reversible and irreversible behavior of this domain wall movement can be described by the Rayleigh law.[27–35] If an alternating electric field is applied with peak amplitudes (E_0) approximately up to $\frac{E_c}{2}$, 50% of the coercive field (E_c), the real nonlinear permittivity and piezoelectric coefficients can be described by

$$\varepsilon' = \varepsilon'_{init} + \alpha'_\varepsilon E_0, \tag{3}$$

$$d' = d'_{init} + \alpha'_d E_0, \tag{4}$$

where ε' and d' are the real relative permittivity and piezoelectric coefficient, ε'_{init} and d'_{init} are the reversible permittivity and piezoelectric coefficient, and α'_ε and α'_d are the Rayleigh coefficients. The relative magnitude of $\alpha'_{\varepsilon,d}$ is a measure of the extrinsic domain wall contribution to piezoelectric and dielectric properties of ferroelectric materials.[29] The real permittivity at each applied electric field is extracted from the polarization-field loop from the peak value and the loop area.[30] An analogous approach can be used to describe both the direct and converse piezoelectric responses. The details of the Rayleigh analysis technique for the dielectric and converse piezoelectric response in ferroelectric materials have been described previously.[29] The Rayleigh parameters and associated errors were obtained from least-squares fitting to the linear portion of the real field dependent response.

D. Microscopy

TEM specimens were prepared from poled samples with the poling direction perpendicular to the column axes. Samples were manually thinned to 20–30 μm and affixed to copper grids using a two-part epoxy. Mechanically thinned samples were thinned to electron transparency using an ion mill (Fisichone) using argon and liquid nitrogen cooling to limit heating and lead loss. Samples were observed on a TEM (EM420, Philips Electron Optics) operating at 120 keV

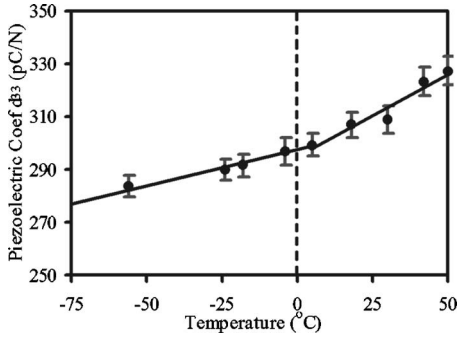

FIG. 4. Temperature dependence of high field unipolar piezoelectric response d_{33} for PZT 60/40. Error bars indicate 95% confidence bands from linear regression analysis.

using an *in situ* dual tilt cold stage (Gatan) and applying diffraction contrast methods.

III. RESULTS AND DISCUSSION

A. Electrical characterization

Initial electromechanical properties were measured on poled disks using the piezoelectric resonance method described above. Low-field resonance data were obtained on the poled PZT ceramics as a function of temperature in both the $R3c$ and $R3m$ phases. Figures 3(a)–3(d) summarize the results from planar and thickness resonance modes. In both 30 and 40 mol % titanium samples a discontinuity in the electromechanical coupling coefficients (k_p, k_t) and radial frequency coefficient (N_p) is observed near the reported tilt transition temperature (T_{tilt}=75 °C and T_{tilt}=0 °C, respectively). High-field behavior was accessed under large unipolar electric fields (20 kV/cm) for 30 mol % titanium samples in the temperature range of the tilt transition. The unipolar piezoelectric coefficient (d_{33}) shows an increase in the temperature dependence of the response above the tilt transition temperature (T_{tilt}=0 °C), as indicated in Fig. 4. The data for the 30 mol % PT samples is in good agreement with the points obtained from bulk samples in the PZT phase diagram. The inflection point in both the resonance and unipolar measurements for the 40 mol % titanium samples suggests that the tilt transition temperature is 0 °C. This result is in good agreement with the tilt transition temperature which would be extrapolated from the accepted PZT phase diagram, after Jaffe *et al.*[36] This temperature, however, is higher than the results reported based on earlier TEM investigations.[13] The expected local temperature deviations from thermocouple reading in the *in situ* TEM stage may explain the difference in the transition temperature between bulk and TEM results.

Using a simple Landau theory the approximate temperature dependence of the intrinsic piezoelectric response can be obtained according to the relationship

$$d = 2Q\varepsilon_r'\varepsilon_0 P, \tag{5}$$

where Q is the electrostrictive coefficient, ε_r' is real relative permittivity, ε_0 is the permittivity of free space, and P is the

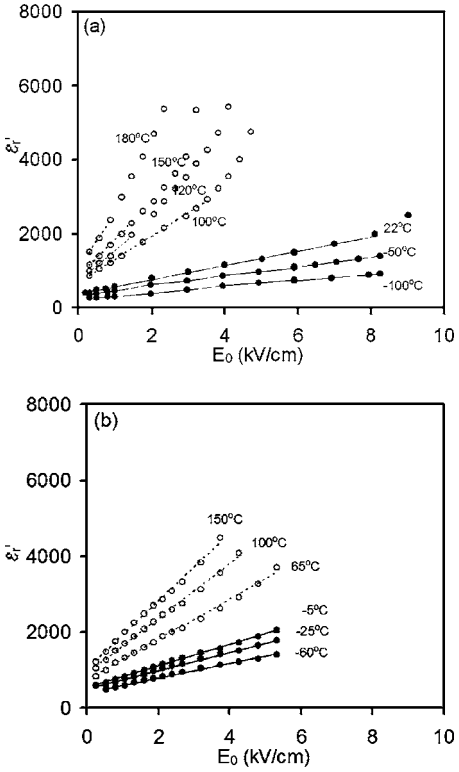

FIG. 5. Nonlinear dielectric response indicates increased field dependence in the untilted phase (dotted lines) for PZT compositions with x=30 (a) and 40 (b) mol % Zr content.

remanent polarization.[37–39] The electrostrictive coefficient can be assumed to be largely temperature independent.[37,38,40] From this relationship, the temperature dependence of the intrinsic piezoelectric response is expected to follow that of the permittivity and polarization—i.e., $d(T) \propto (T_c\text{-}T)^{-1/2}$ where T_C is the Curie temperature.[40] In the temperature range studied here the temperature dependence of the intrinsic response is therefore expected to be small, as we are far from T_C. Furthermore, careful dielectric and pyroelectric measurements revealed no anomaly or change in temperature dependence near the tilt transition temperature. It can be concluded that the change in both the low- and high-field piezoelectric response at the tilt transition temperature is primarily due to a change in the extrinsic contribution.

In order to quantify the change in magnitude of the extrinsic response at the tilt transition, subswitching dielectric hysteresis loops were investigated following the Rayleigh technique. Rayleigh measurements were used to probe the dynamic domain wall motion and extrinsic contribution to the dielectric permittivity. The temperature dependence of the nonlinear dielectric response is shown in Figs. 5(a) and 5(b) both above and below the $R3m$ to $R3c$ tilt transition temperature (T_{tilt}, indicated by a dotted line). In the untilted phase ($T > T_{tilt}$) both compositions show greater field dependence of the total complex dielectric response. Following the Rayleigh fitting procedure described above, the temperature dependence of the dielectric Rayleigh coefficients is shown in Figs. 6(a) and 6(b). The $R3c$ phases below the octahedral tilt transition temperature have smaller and relatively temperature-independent α coefficients. However, above the

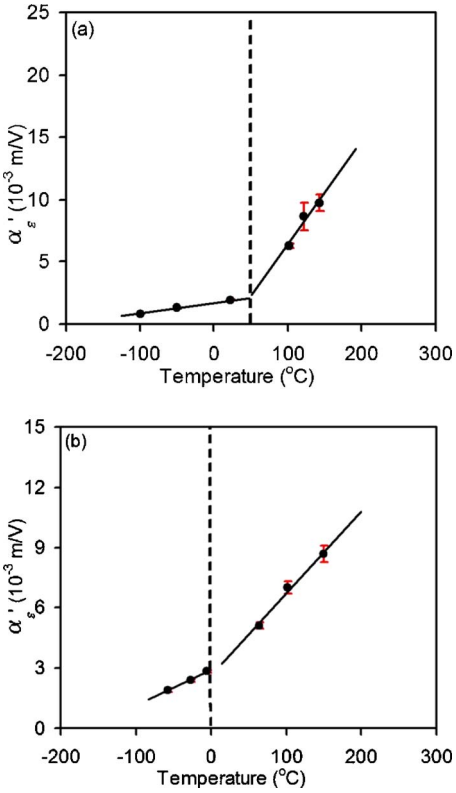

FIG. 6. (Color online) The temperature dependence of Rayleigh slope parameters for PZT compositions, with $x=30$ (a) and 40 (b) mol % Zr content, shows a clear enhancement in field dependence of both the dielectric response above the tilt transition temperature. Error bars indicate 95% confidence bands from linear regression analysis.

tilt transition temperature α coefficients show an increasing temperature dependence. This discontinuity in the temperature dependence of the extrinsic response is consistent with a suppression of domain wall motion below the tilt transition temperature. Similar to the field dependent α term, the low field Rayleigh coefficients ε'_{init} also reveals a discontinuity near tilt transition temperature. The initial permittivity coefficient values are also suppressed in the tilted phase as illustrated for the $Pb(Zr_{0.7},Ti_{0.3})O_3$ composition in Fig. 7. These initial permittivity values may include both intrinsic and reversible domain wall motion contributions to the permittivity. The suppression of the dielectric response, using the Rayleigh method, in both the field dependent (α) and low field (ε_{init}) terms, is summarized in Table I. Rayleigh analysis results are consistent with large domain contributions to both the high-field and low-field response. Although not shown here, similar changes were observed in the Rayleigh analysis of the converse piezoelectric response. Both Rayleigh coefficients (α_d and d_{init}) and the temperature dependence are higher in the $R3m$ phase relative to the $R3c$ phase.

B. Transmission electron microscopy study

Doubling of the unit cell, illustrated previously in Fig. 2, gives rise to superlattices associated with variants of the $R3c$ phase.[23] These are $h+\frac{1}{2}$, $k+\frac{1}{2}$, and $\ell+\frac{1}{2}$ spots relative to the

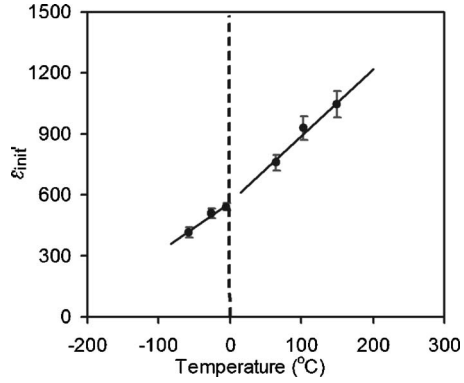

FIG. 7. The low-field or initial permittivity values (ε^*_{init}) indicate a change in slope at the tilt transition temperature, as shown for the 30 mol % Zr PZT composition. Error bars indicate 95% confidence bands from linear regression analysis.

pseudocubic positions. Zone axis electron diffraction in ⟨110⟩ and ⟨211⟩ type zones enables the detection of these octahedral tilt superlattice reflections. Tilting the crystallite orientation to systematic rows containing those reflections and the dark field imaging of the superlattice reflections enables the antiphase boundaries (APB's) to be imaged together with the ferroelectric 71°, 109°, and 180° domain boundaries.[22,23] Figure 8 shows a dark field image containing ferroelectric domain walls and APB's. A calculated [211] zone axis is also provided, for reference, showing the superlattice reflections associated with antiphase tilts along a threefold axis [111]. By combining bright and dark field conditions, imaging transmitted and diffracted beams, we conclude that often the APB's from tilt variance run parallel to the non-180° ferroelectric domains (109° or 71° domains). The inset illustrates a possible tilt variance and the strain discontinuity across the APB's, in this case a change in the stacking sequence of oppositely tilted layers.

TABLE I. Summary of Rayleigh coefficients calculated for PZT compositions above and below the tilt transition temperature.

Temperature (°C)	Phase	α'_ε (10^{-3} m/V)	ε'_{init}
$Pb(Zr_{0.70},Ti_{0.30})O_3$			
−100	tilted	0.84	233
−50	tilted	1.31	323
23	tilted	1.91	377
101	untilted	6.27	665
122	untilted	8.6	689
143	untilted	9.74	842
180	untilted	14.8	1043
$Pb(Zr_{0.60},Ti_{0.40})O_3$			
−58	tilted	1.91	415
−27	tilted	2.4	510
−5	tilted	2.84	541
64	untilted	5.13	758
102	untilted	7.02	929
150	untilted	8.66	1043

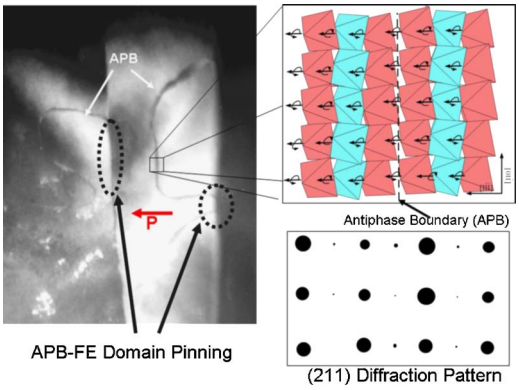

FIG. 8. (Color online) Diffraction contrast image of $Pb(Zr_{0.30},Ti_{0.70})O_3$ taken using transmitted and $(\frac{1}{2},\frac{1}{2},\frac{1}{2})$ superstructure reflections in the [211] zone axes (lower right, calculated CaRIne). The locations of the antiphase boundaries (APB's) are indicated as are regions in which the APB's are pinned at ferroelectric domain boundaries. A possible variance across the APB's is illustrated in the inset (upper right).

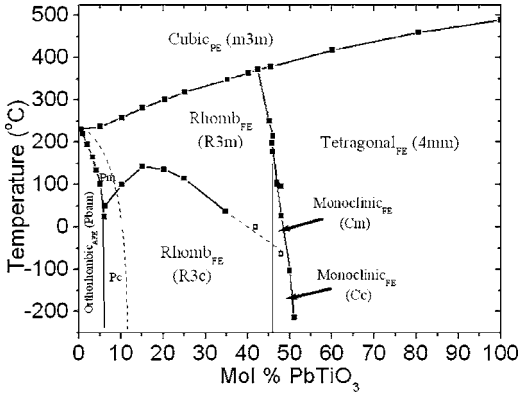

FIG. 9. A self-consistent $PbZrO_3$-$PbTiO_3$ phase diagram has been compiled from a number of sources to include complete space group details (Refs. 10–15, 55, and 56). Open squares indicate revised data points for the position of the *R*3*m*-*R*3*c* transition (current work) and *Cm*-*Cc* transition (after Hatch *et al.*) confirming the tilt boundary (dashed line) is continuous across the rhombohedral-monoclinic phase boundary (Ref. 14).

C. Discussion

The Rayleigh law was originally developed to describe the nonlinear induced magnetization of ferromagnetic materials with increasing applied magnetic field.[41] Néel confirmed mathematically that the Rayleigh response is consistent with the motion of an interface through a random energy potential, as would arise from the motion of ferromagnetic domain walls through pinning defects.[42,43] The literature sited previously confirms that the Rayleigh law is applicable to the study of ferroelectric materials. The Rayleigh data presented in the current work quantify the enhancement of domain wall contributions in the untilted phase. By analogy to Néel's proof and the large body of ferromagnetic literature, this is consistent with the existence of additional or larger pinning sites in the tilted phase of a ferroelectric material.

The formation of ferroelectric and ferroelectric (tilt) domains satisfies thermodynamic conditions which reduce the free energy due to both electric and elastic boundary conditions. Different parts of the domain wall may require different activation energy and experience different domain wall mobility. Regions with lower mobility and higher activation energy will limit the overall extrinsic response of the whole crystallite. As indicated in the TEM micrograph in some areas the APB's and non-180° domain walls are coincident. The formation of these regions likely minimizes the local strain energy in the interior of the crystal. The strain mismatch between each tilt variant may reduce domain mobility and increase activation energy. In this case these coincident regions would be the most difficult to move under external stress and restrict ferroelectric domain wall motion.

Taken together the Rayleigh and TEM results suggest that the APB's act as pinning sites to ferroelectric domain wall motion, suppressing the extrinsic response in the octahedrally tilted phase. This finding has considerable impact concerning the design and discovery of piezoelectric materials with enhanced piezoelectric properties. A specific family of interest is the high-temperature piezoelectric system based on $BiMO_3$-$PbTiO_3$ solid solutions, where *M* may be one or more metal cations in a stoichiometric ratio to give an average $\langle +3 \rangle$ valence to the octahedral site.[44–51] In polycrystalline piezoelectric ceramics, the highest piezoelectric properties are found within solid solutions close to the MPB between tetragonal and rhombohedral ferroelectric phases analogous to the PZT system. Untilted MPB compositions in these systems have been reported with Curie temperature exceeding PZT and piezoelectric coefficient $d_{33} > 400$ pC/N, for example $BiScO_3$-$PbTiO_3$.[44] However, the authors and others have observed that a number of octahedral tilt systems exist in and around the MPB phase in other bismuth-perovskite–lead titanate systems—for example, $Bi(Mg_{1/2},Ti_{1/2})O_3$-$PbTiO_3$.[52–54] The measured piezoelectric properties of several bismuth perovskite systems near the MPB are often half those of $BiScO_3$-$PbTiO_3$ for compositions with similar paraelectric-ferroelectric transition temperatures at the MPB ($T_C \sim 450$ °C). Although not all these systems have been fully analyzed and characterized for tilt, tilted ferroelectric-ferroelastic MPB phases clamping extrinsic contributions to the piezoelectric response would explain their poor performance relative to the $BiScO_3$-$PbTiO_3$ system.

IV. SUMMARY AND CONCLUSIONS

Electromechanical property investigation and TEM structural analysis in the PZT system were combined in order to study the role of octahedral tilt transitions on the dielectric and piezoelectric properties of technologically important ferroelectric ceramic compositions. In order to avoid contributions associated with the structural complexities near the MPB, the temperature dependence of properties across the tilt transition were measured in two PZT compositions with rhombohedral structure at room temperature. Both low-field electromechanical resonance measurements and high-field

unipolar strain measurements revealed a shift in properties near the temperature of the octahedral phase transition. Specifically, a discontinuity in the temperature dependence was observed at ~75 °C and ~0 °C in the $x=30$ and 40 mol % zirconium compositions, respectively. From this work the phase diagram of the PZT system has been revised to extend the $R3c$-$R3m$ phase boundary to higher lead titanate content, as shown in Fig. 9.[10–15,55,56]

The origin and magnitude of this change in properties were then quantified using Rayleigh analysis. The Rayleigh law response indicated that the relative magnitude of the ferroelectric domain contribution to both the dielectric and piezoelectric response was suppressed in PZT compositions in the tilted region of the phase diagram. The microstructural features identified in the $R3c$ phase field were consistent with the literature and confirm an interaction between octahedral APB's and ferroelectric domain walls. When coupled with electromechanical property data a clear association is drawn between the interaction of the APB's with domain walls and the suppression of electromechanical properties in tilted ferroelectrics. This result has broad implications for the application and development high-performance piezoelectric materials, as was discussed for the case of the $BiMO_3$-$PbTiO_3$ systems.

*Present address: Department of Chemical and Materials Engineering, University of Kentucky, Lexington, KY 40506, USA.

[1] F. S. Galasso, *Structure, Properties, and Preparation of Perovskite-Type Compounds* (Pergamon Press, New York, 1969).
[2] *Perovskite: A Structure of Great Interest to Geophysics and Materials Science*, edited by A. Navrotsky and D. J. Weidner (American Geophysical Union, Washington, D.C., 1989).
[3] X. L. Zhang, Z. X. Chen, L. E. Cross, and W. A. Schulze, J. Mater. Sci. **18**, 968 (1983).
[4] V. D. Kugel and L. E. Cross, J. Appl. Phys. **84**, 2815 (1998).
[5] Q. M. Zhang, H. Wang, N. Kim, and L. E. Cross, J. Appl. Phys. **75**, 454 (1994).
[6] D. Damjanovic and M. Demartin, J. Phys.: Condens. Matter **9**, 4943 (1997).
[7] C. A. Randall, N. Kim, J. P. Kucera, W. W. Cao, and T. R. Shrout, J. Am. Ceram. Soc. **81**, 677 (1998).
[8] G. Arlt, H. Dederichs, and R. Herbiet, Ferroelectrics **74**, 37 (1987).
[9] R. Herbiet, U. Robels, H. Dederichs, and G. Arlt, Ferroelectrics **98**, 107 (1989).
[10] H. M. Barnett, J. Appl. Phys. **33**, 1606 (1962).
[11] B. Jaffe, R. S. Roth, and S. Marzullo, J. Appl. Phys. **25**, 809 (1954).
[12] B. Noheda, J. A. Gonzalo, L. E. Cross, R. Guo, S.-E. Park, D. E. Cox, and G. Shirane, Phys. Rev. B **61**, 8687 (2000).
[13] D. I. Woodward, J. Knudsen, and I. M. Reaney, Phys. Rev. B **72**, 104110 (2005).
[14] D. M. Hatch, H. T. Stokes, R. Ranjan, Ragini, S. K. Mishra, D. Pandey, and B. J. Kennedy, Phys. Rev. B **65**, 212101 (2002).
[15] C. Michel, J. M. Moreau, Achenbac. Gd, R. Gerson, and W. J. James, Solid State Commun. **7**, 865 (1969).
[16] M. E. Lines and A. M. Glass, *Principles and Applications of Ferroelectrics and Related Materials* (Clarendon Press, Oxford, 1977).
[17] A. M. Glazer, Acta Crystallogr., Sect. B: Struct. Crystallogr. Cryst. Chem. **28**, 3384 (1972).
[18] A. M. Glazer, Acta Crystallogr., Sect. A: Cryst. Phys., Diffr., Theor. Gen. Crystallogr. **31**, 756 (1975).
[19] D. I. Woodward and I. M. Reaney, Acta Crystallogr., Sect. B: Struct. Sci. **61**, 387 (2005).
[20] H. Zheng, I. M. Reaney, and W. E. Lee, J. Am. Ceram. Soc. **85**, 2337 (2002).
[21] H. Zheng, I. M. Reaney, W. E. Lee, N. Jones, and H. Thomas, Ferroelectrics **268**, 125 (2002).
[22] C. A. Randall, M. G. Matsko, W. Cao, and A. S. Bhalla, Solid State Commun. **85**, 193 (1993).
[23] J. Ricote, D. L. Corker, R. W. Whatmore, S. A. Impey, A. M. Glazer, J. Dec, and K. Roleder, J. Phys.: Condens. Matter **10**, 1767 (1998).
[24] D. Viehland, J. F. Li, X. H. Dai, and Z. Xu, J. Phys. Chem. Solids **57**, 1545 (1996).
[25] U. Robels, R. Herbiet, and G. Arlt, Ferroelectrics **93**, 95 (1989).
[26] C. A. Randall, D. J. Barber, and R. W. Whatmore, J. Mater. Sci. **22**, 925 (1987).
[27] D. Damjanovic and M. Demartin, J. Phys. D **29**, 2057 (1996).
[28] D. Damjanovic and D. V. Taylor, Ferroelectrics **221**, 137 (1999).
[29] R. E. Eitel, T. R. Shrout, and C. A. Randall, J. Appl. Phys. **99**, 124110 (2006).
[30] N. B. Gharb and S. Trolier-McKinstry, J. Appl. Phys. **97**, 064106 (2005).
[31] D. A. Hall, J. Mater. Sci. **36**, 4575 (2001).
[32] D. A. Hall, M. M. Ben-Omran, and P. J. Stevenson, J. Phys. D **10**, 461 (1998).
[33] D. A. Hall and P. J. Stevenson, Ferroelectrics **228**, 139 (1999).
[34] D. V. Taylor and D. Damjanovic, Appl. Phys. Lett. **73**, 2045 (1998).
[35] D. V. Taylor, D. Damjanovic, and N. Setter, Ferroelectrics **224**, 727 (1999).
[36] B. Jaffe, W. R. Cook, and H. Jaffe, *Piezoelectric Ceramics* (Academic Press, New York, 1971).
[37] M. J. Haun, Ph.D. Thesis, The Pennsylvania State University, 1988.
[38] M. J. Haun, E. Furman, S. J. Jang, H. A. McKinstry, Z. Q. Zhuang, T. R. Halemane, and L. E. Cross, Ferroelectrics **99**, 13 (1989).
[39] G. A. Rossetti, L. E. Cross, and J. P. Cline, J. Mater. Sci. **30**, 24 (1995).
[40] K. Uchino, *Ferroelectric Devices* (Marcel Dekker, Inc., New York, 2000).
[41] L. Rayleigh, Philos. Mag. **23**, 225 (1887).
[42] L. Néel, Cah. Phys. **12**, 1 (1942).
[43] L. Néel, Cah. Phys. **13**, 18 (1943).
[44] R. E. Eitel, C. A. Randall, T. R. Shrout, and S. E. Park, Jpn. J. Appl. Phys., Part 1 **41**, 2099 (2002).
[45] R. E. Eitel, C. A. Randall, T. R. Shrout, P. W. Rehrig, W. Hack-

enberger, and S. E. Park, Jpn. J. Appl. Phys., Part 1 **40**, 5999 (2001).
[46] M. R. Suchomel and P. K. Davies, Appl. Phys. Lett. **86**, 262905 (2005).
[47] T. H. Song, R. E. Eitel, T. R. Shrout, and C. A. Randall, Jpn. J. Appl. Phys., Part 1 **43**, 5392 (2004).
[48] T. H. Song, R. E. Eitel, T. R. Shrout, C. A. Randall, and W. Hackenberger, Jpn. J. Appl. Phys., Part 1 **42**, 5181 (2003).
[49] S. M. Choi, C. J. Stringer, T. R. Shrout, and C. A. Randall, J. Appl. Phys. **98**, 034108 (2005).
[50] Y. Inaguma, A. Miyaguchi, M. Yoshida, T. Katsumata, Y. Shimojo, R. P. Wang, and T. Sekiya, J. Appl. Phys. **95**, 231 (2004).
[51] C. J. Stringer, R. E. Eitel, T. R. Shrout, C. A. Randall, and I. M. Reaney, J. Appl. Phys. **97**, 024101 (2005).
[52] C. A. Randall, R. Eitel, B. Jones, T. R. Shrout, D. I. Woodward, and I. M. Reaney, J. Appl. Phys. **95**, 3633 (2004).
[53] C. A. Randall, R. E. Eitel, T. R. Shrout, D. I. Woodward, and I. M. Reaney, J. Appl. Phys. **93**, 9271 (2003).
[54] D. I. Woodward, I. M. Reaney, R. E. Eitel, and C. A. Randall, J. Appl. Phys. **94**, 3313 (2003).
[55] B. Jaffe, J. Res. Natl. Bur. Stand. **55**, 239 (1955).
[56] H. Jaffe and D. A. Berlincourt, Proc. IEEE **53**, 1372 (1965).